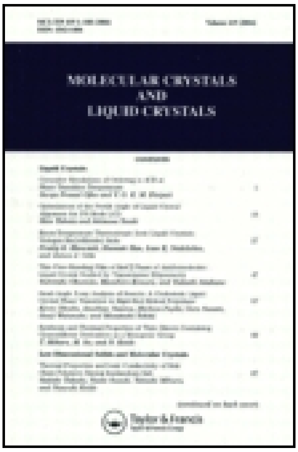

Molecular Crystals and Liquid Crystals
Publication details, including instructions for authors and subscription information:
http://www.tandfonline.com/loi/gmcl20

Light Propagation Through Alignment-patterned Liquid Crystal Gratings

Toralf. Scharf [a] & Christian Bohley [a]

[a] Institute of Microtechnology, University of Neuchâtel, Rue A.-L. Breguet 2, Neuchâtel, 2000, Switzerland

Version of record first published: 18 Oct 2010

To cite this article: Toralf. Scharf & Christian Bohley (2002): Light Propagation Through Alignment-patterned Liquid Crystal Gratings, Molecular Crystals and Liquid Crystals, 375:1, 491-500

To link to this article: http://dx.doi.org/10.1080/10587250210589

Mol. Cryst. Liq. Cryst., Vol. 375, pp. 491-500

1058-725X/02 $12.00 + .00

Light Propagation Through Alignment-patterned Liquid Crystal Gratings

TORALF. SCHARF and CHRISTIAN BOHLEY

Institute of Microtechnology, University of Neuchâtel, Rue A.-L. Breguet 2, 2000 Neuchâtel, Switzerland

We analysed the light propagation through alignment-patterned liquid crystal films where the alignment is planar and homeotropic for different domains, respectively. Using elastic theory the nematic director field can be analytically calculated with the method of conformal mapping in the one elastic constant approximation. A smooth change of the nematic director field is found with defect points at the substrate surfaces. In order to investigate the propagation of light passing through such a liquid crystalline thin film with spatially varying birefringence, we use a rigorous method. The use of rigorous methods allows the simulation of the time-dependent electric and magnetic fields for a region that is two-dimensional and possibly anisotropic. Simulations are made by the finite-difference time-domain method (FDTD), which is a numerical approach for the rigorous solution of the Maxwell equations. This method, in contrast to methods of geometrical and matrix optics, delivers results which include diffraction and scattering.

Keywords: Liquid crystal gratings, anisotropic gradient index media, light propagation, finite-difference time-domain method

INTRODUCTION

Recently, liquid crystal displays with multi-domain alignment were developed [1]. They show interesting optical properties concerning viewing angle and polarization of light. Polarization insensitive spatial light modulators [1, 2] have very high efficiencies when used as switchable gratings and beam deflectors. Anyhow by increasing the spatial resolution of the alignment-pattern the liquid crystal director field becomes a gradient one and defects appear. The light propagation through such anisotropic gradient refractive index system is not anymore easy to handle especially if the director configurations contain twist deformation. Here we want to discuss planar oriented liquid crystal director fields without any twist distortion. They serve as general model systems for anisotropic gradient index gratings. The alignment will be patterned with homeotropic and planar alignment under strong anchoring conditions. In that case an analytical model allows calculation of the director profile [3-5] in the one constant approximation and the light propagation can be simulated by different methods afterwards. For a constant thickness of the liquid crystal film the sizes of the surface alignment-patterned part are changed to detect differences in light propagation. We use Berreman matrix method [6, 7] to compare the simulations made with a finite-difference time-domain method [8]. The far field and the diffraction efficiencies are calculated. The diffraction properties of a periodic arrangement of such structures are explored by propagating the emerging light in the far field.

SIMULATION OF THE DIRECTOR FIELD

When two adjacent regions on a substrate surface of a nematic liquid crystal cell are subjected to different anchoring conditions, the boundary between the two regions constitutes a disclination line attached to the surface substrate, i.e. a surface disclination. Disclinations sticking at a solid-nematic interface also occur when the substrate is not flat or has sharp corners or edges. The director configurations around the surface disclinations associated with modified flat substrates can be analysed using a function theoretical method [3, 5]. In that what follows we assume that the director field is two-dimensional; the state of alignment in the liquid crystal cell depends only on the x and y coordinates, i.e. the director **n** is in the (x,y)-plane. We assume that the surface anchoring of the liquid crystal is always strong.

Consider a cell in which the liquid crystal is confined between two parallel-plate substrates, the distance between the two plates being d. Let the x axis lie in the lower substrate, the y axis being perpendicular to that plane as shown in Figure 1. The director **n** is in the (x,y) plane and forms an tilt angle $\phi(x,y)$ with the x-axis:

$$\mathbf{n} = (\cos\phi, \sin\phi, 0) \tag{1}$$

We impose the boundary conditions for the director so that we have on one substrate surface uniform alignment and on the other a modified substrate as shown in Figure 1. The alignment conditions change from homeotropic to planar and from planar to homeotropic at positions $x = -a$ and $x = a$, respectively.

In the one constant approximation [9] the distortion free energy F of the cell is given by

$$F = \frac{1}{2} K \iint \left[(\partial\phi/\partial x)^2 + (\partial\phi/\partial y)^2 \right] dx\, dy \tag{2}$$

where K is the elastic constant. The equilibrium director configuration, in which F is minimal, must satisfy the two-dimensional Laplace equation

$$\partial^2\phi/\partial x^2 + \partial^2\phi/\partial y^2 = 0 \tag{3}$$

subjected to the boundary conditions. One now introduces a complex variable $z = x + iy$ and considers a regular function Φ in the complex z plane. Then the real and imaginary parts of Φ are harmonic functions satisfying the Laplace equation Eq. 3. Here we assume that the imaginary part of Φ satisfies the given boundary conditions. However,

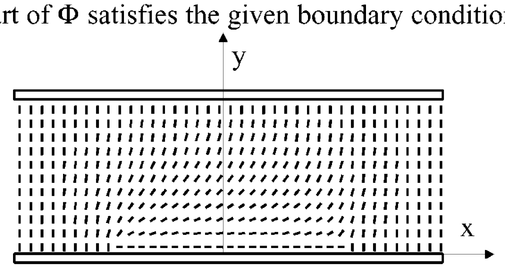

FIGURE 1 Nematic director field for a liquid crystal cell of modified substrates with one alignment-patterned surface. The planar alignment is imposed on the lower substrate from $x = -a$ to $x = a$.

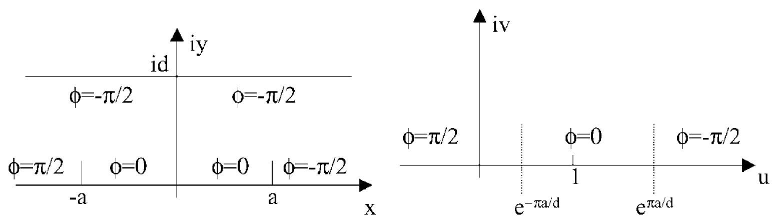

FIGURE 2 The complex z- and w-plane with boundary conditions before and after conformal mapping.

in general, it is not an easy task to determine the required regular function directly. Therefore one uses the method of conformal mapping [10]. By means of a suitable regular function $w = f(z) = u + iv$ one maps the domain $0 \leq y \leq d$ of the complex z-plane conformal onto the upper half of the complex w-plane. If we can find a regular function $\Psi(w)$ in the w-plane which satisfies the boundary condition in the w-plane than transforming back into the original z-plane we have the required solution $\varphi(x, y)$ of the boundary value problem as the imaginary part of $\Phi(z) = \Psi(f(z)) = \psi(x, y) + i\varphi(x, y)$.

Having stated the method, let us now proceed to solve the given boundary value problem. The relevant transformation is $w = \exp(\pi z/d)$ which maps the x-axis $(y = 0)$ and the line $y = d$ onto the u-axis, as shown in Figure 2. In the w-plane a regular function, whose imaginary part is compatible with the boundary conditions is found by inspection to be

$$\Psi(w) = 1/2 \cdot \left(\log\left(w - e^{-\pi a/d}\right) - \log\left(e^{\pi a/d} - w\right)\right) \tag{4}$$

This is because the logarithm function for complex variables $\log(z) = \ln|z| + i\arg(z)$ changes the imaginary part from 0 to π when changing the variable z from positive to negative values, i.e. $\mathrm{Im}(\log(-a)) = \pi$ and $\mathrm{Im}(\log(a)) = 0$ for a real and $a > 0$. The distinction between the director positions θ and $\theta \pm \pi$ is irrelevant for the tilt angle of the nematic liquid crystal director [9]. Therefore there are different possibilities to create the boundary conditions and functions $\Psi(w)$ that fulfill these boundary conditions. Different director configurations are possible, where one is the energetically favourable. The configuration shown in Figure 1 is the one with the lowest free energy [3, 5].

Backward transformation of the found function $\Psi(w)$ gives

$$\Phi(z) = \Psi\left(e^{\pi z/d}\right) = 1/2 \cdot \left(\log\left(e^{\pi z/d} - e^{-\pi a/d}\right) - \log\left(e^{\pi a/d} - e^{\pi z/d}\right)\right) \tag{5}$$

After simplification one finds finally the tilt angle profile $\phi(x, y)$ as the imaginary part of $\Phi(z)$. That is

$$\phi(z) = 1/2 \cdot \arctan\left(\frac{\sin(\pi y/d)\sinh(\pi a/d)}{\cos(\pi y/d)\cosh(\pi a/d) - \cosh(\pi x/d)}\right) \tag{6}$$

The model allows the extension to gratings with more than one period. Using Eq. (6) we are now able to calculate director configurations for arbitrary cell thickness and sizes of the alignment patterned structure. For increasing sizes of the alignment-patterned structures the influence of the planar alignment becomes stronger and in the limit of infinite large structures the director configuration is hybrid.

LIGHT PROPAGATION SIMULATION

Anisotropic gradient index media are difficult to handle with conventional light propagation simulation methods like ray tracing. To handle a gradient index distribution of a birefringent uniaxial media is a great problem of the optics including anisotropy. In a previous study [11] we found that the limit of spatial resolution of alignment-patterned gratings is given by the thickness of the liquid crystal layer. Experimental results and simulations proved that a simple Jones matrix calculation is not sufficient to understand the optical properties of such spatial resolution-limited gratings because of strong gradients in the refractive index distribution.

In order to investigate the propagation of light passing through a liquid crystalline structure of micrometer size we use a rigorous method. This allows the simulation of the time-dependent electric and magnetic fields for a region that is two-dimensional and possibly anisotropic. For the director profile described above in the previous chapter, the condition for which the problem can be separated in TE and TM polarizations is fulfilled. This is because the Maxwell equations for such a problem decouple for two perpendicular linear polarizations.

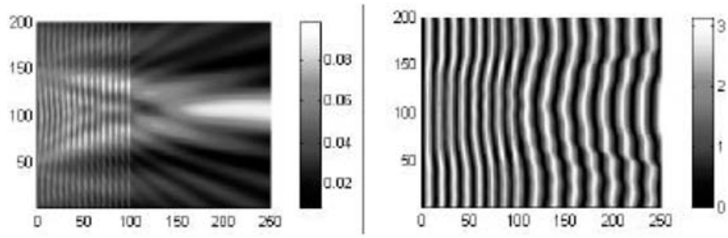

FIGURE 3 Intensities and Phases of light propagating through structure shown in Figure 1 with FDTD anisotropic method

Simulations are made by the finite-difference time-domain method (FDTD) [8], which is a numerical approach for the rigorous solution of the Maxwell equations. The perfectly matched layer (PML) boundary conditions were used to avoid disturbing reflection form the borders of the simulation box. The FDTD method, in contrast to the methods of geometrical and matrix optics, delivers results which include diffraction and scattering. As an example, Figure 3 shows an amplitude and phase distribution for TM polarization at a wavelength of 550 nm. The corresponding director profile is shown in Figure 1. The spatial distribution of the birefringence causes a focalisation of the intensity and the phase is modulated. The simulation box is 5.5μm high and 6.875 μm wide with a discretization of 20 points per wavelength. The liquid crystal layer has a thickness of 2.75 μm and the regions where the liquid crystal and the air are present are distinguishable via the smaller period of the wave field in the medium with higher refractive index, i.e. the liquid crystal

To compare different optical simulation techniques we calculate the amplitude and phase profiles at the exit of the liquid crystal structure with three different methods and plot the results in Figure 4. Seeing that the director configuration has no twist distortion, the polarizations are separable and the incident linear polarised light stays linear polarized but undergoes a certain phase shift and amplitude modulation. The amplitudes and phases in Figure 4 are shown for incident linear polarization with the polarization direction lying in the paper plane (TM). The rigorous simulations including anisotropy are compared with the Berreman matrix method and a rigorous simulation with assumed isotropy. The refractive index gradient profile for the isotropic FDTD is found by calculating an effective refractive index for each point of discretization for the direction normal to the substrate surfaces. The isotropic approach with the FDTD method allows taking the gradient into account and their performance can be compared with advanced polarization ray tracing methods [12].

Comparing first the amplitude profiles on the right of Figure 4 one sees immediately remarkable differences in the amplitude distribution. For the Berreman Matrix method a very low modulation of the intensity becomes visible because for the Berreman matrix calculation, intensity modulation only happens in the region of very

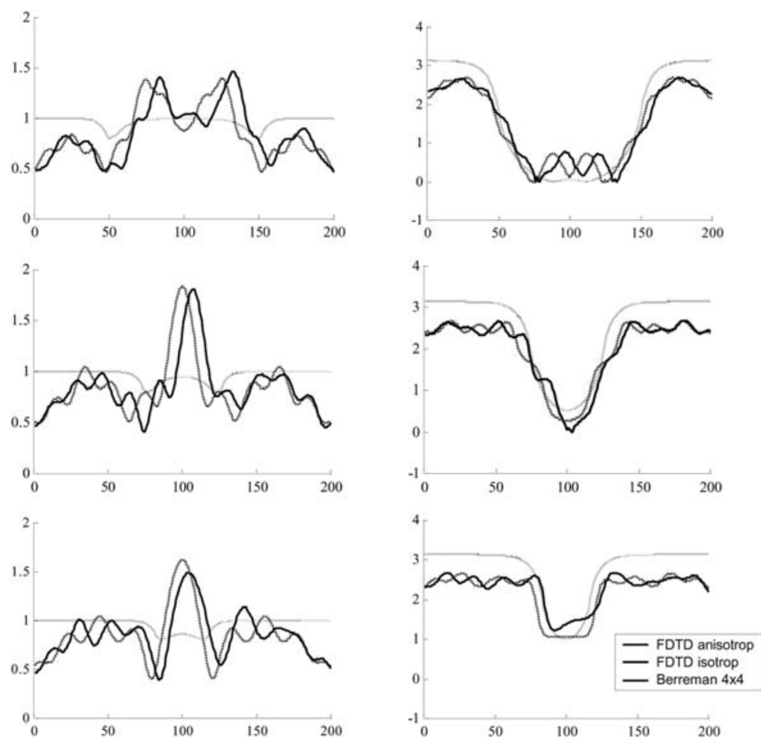

FIGURE 4 Amplitude and phase for the different sizes and methods. The size of the alignment-patterned part is changed from d, 0.5d to 0.25d. The graphs show the results for a 4x4 Berreman method, gradient index method with an effective index and the rigorous anisotropic simulations.

strong distorted nematic director fields. The rigorous methods show amplitude variations of more than 50% due to the influence of the gradient in the birefringent distribution. Beside this, the Berreman method and the gradient index calculation without anisotropy give symmetric distributions of amplitude and phases and only the rigorous method including anisotropy shows the expected asymmetry. An asymmetry with respect to the y-axis of the director field is given and is only recognized by the FDTD method. In general, the phase profiles differ not much and it could be concluded that the difference between the calculated light propagation models lies in the pronounced amplitude distribution.

The main criteria to characterize such structures if they are arranged in gratings are the diffraction efficiencies. For comparison we calculated the diffraction efficiencies with Fraunhofer approximation [13] by Fourier transform the complex amplitudes shown in Figure 4. It is clear that this could give us just an indication of the problem of the spatial resolution limit of liquid crystal alignment-patterned gratings because the director configuration for a single pixel of planar oriented liquid crystal and a grating of such structures will not be the same. Nevertheless, in good approximation we can accept this and we calculated in TABLE 1 the diffraction efficiencies for the different methods of the -2,-1,0,+1,+2 order. Clearly we see that already for a structure size comparable with the thickness of the liquid crystal layer the calculated efficiencies for the matrix method and the rigorous approach differ a lot. Having a look at the zero order intensity for the structure size equal to the thickness d we find for the anisotropic rigorous simulation an intensity in the zero order of I^A_0=0.6. For the isotropic rigorous simulation the intensity in the zero order is I^I_0=0.59 and for the Berreman matrix method we get an intensity of I^B_0=0.06. The diffraction efficiency between the rigorous methods and the matrix method differs by one order of magnitude, which was found in experiments on twisted systems [11]. For smaller structure sizes, the difference is less pronounced because of the general very small diffraction efficiencies with decreasing phase shifts. Remarkable effects coming up for very small structure sizes where the simulation results of all three models differ a lot. At a size structure d/8 the asymmetry of diffraction efficiencies result becomes large and the influence of the anisotropy becomes important. In general, the diffraction efficiencies calculated with the Berreman and the gradient index methods are too large and don't show the correct symmetry.

TABLE 1 Diffraction efficiencies for several orders of alignment-patterned gratings. The structure size is given with respect to the thickness d of the liquid crystal layer. The numbers indicate the positive and negative diffraction orders.

Size	Method \ Diffraction order	-2	-1	0	+1	+2
d	Anisotropic	0.0236	0.0785	0.6003	0.1163	0.0145
	Isotropic	0.0212	0.0998	0.5913	0.0996	0.0210
	Berreman	0.0295	0.3797	0.0553	0.3797	0.0295
d/2	Anisotropic	0.0576	0.1104	0.5374	0.1313	0.0839
	Isotropic	0.0761	0.1255	0.5132	0.1257	0.0761
	Berreman	0.0745	0.1775	0.3961	0.1775	0.0745
d/4	Anisotropic	0.0283	0.0347	0.7302	0.0432	0.0496
	Isotropic	0.0700	0.0725	0.5898	0.0724	0.0700
	Isotropic	0.0492	0.0824	0.6289	0.0824	0.0492
d/8	Anisotropic	0.0040	0.0126	0.8878	0.0162	0.0100
	Isotropic	0.0397	0.0416	0.7194	0.0416	0.0396
	Berreman	0.0302	0.0443	0.7554	0.0443	0.0302

SUMMARY.

We have shown that light propagation in gradient index optical systems with anisotropy has to be handled with rigorous methods of light propagation for structures were the modulated length scale is comparable with the thickness of the cell. That is according to experimental results on liquid crystal gratings with twisted structures and for optical properties on roll instabilities in nematic liquid crystals. A step further is the study of light propagation through anisotropic gradient index media with twist structures. That is much more complicated to handle because of the three-dimensional rigorous calculation necessary. For a diffraction analysis of high-resolution liquid crystal gratings, where the resolution is given by the thickness of the liquid crystal cell, it is not at all sufficient to study a gradient index model or use an approach with Berreman matrix method.

REFERENCE.

[1] C. M. Titus and P. J. Bos, Appl. Phys. Lett., **71**, 2239-2241, (1997).

[2] P. J. Bos, J. Chen, J. W. Deane, B. Smith, C. Holton, and W. Glenn, presented at SID 95 Digest, (1995).

[3] J. A. Geurst, A. M. J. Spruijt, and C. J. Gerritsma, J. de Physique, **36**, 653-664, (1975).

[4] V. Vitek and M. Kléman, J. de Physique, **36**, 59-67, (1975).

[5] K. Okano, K. Kitahara, and E. Ushizawa, Jpn. J. Appl. Phys., **33**, 6262-6267, (1994).

[6] P. Allia, C. Oldano, and L. Trossi, Linear Optics: Matrix Methods, in *Physics of liquid crystalline materials*, I.-C. Khoo and F. Simoni, Eds.: Gordon and Breach, 1991, pp. 337-363.

[7] P. Yeh and C. Gu, Optics of Liquid Crystal Displays. New York: Wiley, (1999).

[8] A. Taflove and S. Hagness, Computational Electrodynamics, second. ed. Norwood: Artech House, (2001).

[9] P. G. d. Gennes and J. Prost, The Physics of Liquid Crystals. Oxford: Clarendon Press, (1995).

[10] R. V. Churchill, Complex Variables and Applications. Tokyo: McGraw-Hill, (1960).

[11] T. Scharf, presented at 29. Arbeitstagung Flüssigkristalle, Freiburg Breisgau, (2000).

[12] J. A. Kosmopoulos and H. M. Zenginoglou, Appl. Opt., **26**, 1714-1721, (1987).

[13] J. W. Goodman, Introduction to Fourier Optics, 2nd International Edition ed. New York: McGraw Hill, (1996).